MCB
Journals.ASM.org

The Ubiquitin E3 Ligase SCF-FBXO24 Recognizes Deacetylated Nucleoside Diphosphate Kinase A To Enhance Its Degradation

Wei Chen,[a] Sheng Xiong,[a] Jin Li,[b] Xiuying Li,[a] Yuan Liu,[b] Chunbin Zou,[b] Rama K. Mallampalli[b,c,d]

Institute of Biomedicine and National Engineering Research Center of Genetic Medicine, College of Life Science and Technology, Jinan University, Guangzhou, China[a]; Department of Medicine, Acute Lung Injury Center of Excellence,[b] and Department of Cell Biology and Physiology,[c] University of Pittsburgh, Pittsburgh, Pennsylvania, USA; Medical Specialty Service Line, Veterans Affairs Pittsburgh Healthcare System, Pittsburgh, Pennsylvania, USA[d]

The Skp-Cul-F box (SCF) ubiquitin E3 ligase machinery recognizes predominantly phosphodegrons or, less commonly, an (I/L)Q molecular signature within substrates to facilitate their recruitment in mediating protein ubiquitination and degradation. Here, we examined the molecular signals that determine the turnover of the multifunctional enzyme nucleoside diphosphate kinase A (NDPK-A) that controls cell proliferation. NDPK-A protein exhibits a half-life of ~6 h in HeLa cells and is targeted for ubiquitylation through actions of the F-box protein FBXO24. SCF-FBXO24 polyubiquitinates NDPK-A at K85, and two NH_2-terminal residues, L55 and K56, were identified as important molecular sites for FBXO24 interaction. Importantly, K56 acetylation impairs its interaction with FBXO24, and replacing K56 with Q56, an acetylation mimic, reduces NDPK-A FBXO24 binding capacity. The acetyltransferase GCN5 catalyzes K56 acetylation within NDPK-A, thereby stabilizing NDPK-A, whereas GCN5 depletion in cells accelerates NDPK-A degradation. Cellular expression of an NDPK-A acetylation mimic or FBXO24 silencing increases NDPK-A life span which, in turn, impairs cell migration and wound healing. We propose that lysine acetylation when presented in the appropriate context may be recognized by some F-box proteins as a unique inhibitory molecular signal for their recruitment to restrict substrate degradation.

The stability of the majority of cellular regulatory proteins is governed by a ubiquitous disposal apparatus, the ubiquitin proteasome system (1). For proteasomal degradation, the selected protein is processed through a hierarchical, highly controlled and relatively selective system involving a series of enzymatic steps. The substrate is ubiquitinated through sequential activities of a ubiquitin-activating enzyme (E1), a ubiquitin-conjugating enzyme (E2), and, finally, a ubiquitin ligase (E3). In the cullin (CUL)-RING ubiquitin ligase superfamily, the E3 complex recognizes a specific substrate by physical interactions using adaptor or receptor-like subunits linked to a scaffold base (2–5). The S-phase kinase-associated protein 1 (Skp1)–cullin 1 (CUL1)–F-box protein (SCF) protein complex is a prototypical multicomponent subfamily of CUL-RING E3 ligases that harbors a key substrate receptor component, the F-box protein, which via Skp1 binds the scaffold protein CUL1. Within the SCF complex, the F-box protein associates with the substrate through its C-terminal substrate binding domain and then binds to Skp1 via its NH_2-terminal F-box domain (5). Depending on the nature of the molecular sequence within the substrate-binding pocket, F-box proteins are categorized into FbxL, FbxW, and FbxO subfamilies.

An important area of investigation is elucidating the molecular signals that recruit the receptor component of SCF-based E3 ligases, the F-box protein, to their targets. It is generally established that phosphorylation within relatively short motifs (phosphodegrons) are key molecular signatures that facilitate the recruitment of F-box proteins to mediate substrate degradation (6). Other less common covalent modifications within substrates that signal recruitment of CUL-RING E3 ligase receptor subunits include glycosylation, methylation, and hydroxylation (7–9). One FbxL family member, F-box protein Fbxl2, recognizes an (I/L)Q motif that serves as a molecular docking site within some substrates, including the phospholipid enzyme cytidylyltransferase, cyclin D2, and cyclin D3 (10–12). While it appears that phosphorylation within degrons can enhance or impede F-box protein binding to a target, unique molecular signals that serve as inhibitory recognition motifs for SCF binding remain largely unknown.

Nucleoside diphosphate kinase A (NDPK-A, encoded by *nm23-H1*) has multiple critical functions apart from its well-known ability to catalyze the conversion of ADP to ATP in the presence of GTP (13). The transferase activity of NDPK-A depends on its histidine protein kinase activity through autophosphorylation. NDPK-A plays an important role in regulating a variety of fundamental cellular processes, including growth and development, G-protein signaling, metastasis, transcriptional regulation, and DNA repair (14, 15). Overexpression of NDPK-A reduces the metastatic potential of highly invasive breast carcinoma and melanoma and prostate, colon, and hepatocellular cancer cells. Numerous proteins involved in critical cellular functions have been identified as potential binding partners with NDPK-A. For example, NDPK-A interacts with and inhibits Tiam1, which acts as a guanine nucleotide exchange factor (GEF) for the Rac1 GTPase, which prevents Rac/Rho activation (16). NDPK-A interacts with Lbc to inactivate RhoA or interacts with Rad to activate Rad and inhibit the Ras pathways (17–20). Hence, interaction with multiple binding

Received 22 September 2014 **Returned for modification** 10 October 2014
Accepted 5 January 2015

Accepted manuscript posted online 12 January 2015

Citation Chen W, Xiong S, Li J, Li X, Liu Y, Zou C, Mallampalli RK. 2015. The ubiquitin E3 ligase SCF-FBXO24 recognizes deacetylated nucleoside diphosphate kinase A to enhance its degradation. Mol Cell Biol 35:1001–1013. doi:10.1128/MCB.01185-14.

Address correspondence to Chunbin Zou, zouc@upmc.edu, or Rama K. Mallampalli, mallampallirk@upmc.edu.

W.C. and S.X. contributed equally to this article.

doi:10.1128/MCB.01185-14

partners is critical for NDPK-A to execute physiologic roles in diverse biological processes (18, 21–23).

As NDPK-A is a key multifunctional and ubiquitously distributed protein, the molecular mechanisms that regulate the enzymatic behavior of NDPK-A by reversible phosphorylation are well described. For example, NDPK-A activity is stringently regulated by 5′ AMP-activated protein kinase (AMPK)-mediated phosphorylation, where AMPKα1 interacts with NDPK-A via E124 to phosphorylate two adjacent residues, S122 and S144 (24–26). AMPK phosphorylates NDPK-A at S122 that augments its enzymatic activity by triggering substrate channeling. NDPK-A is believed to act as a protein kinase to autophosphorylate at H118, a catalytic site within NDPK-A that appears to be critical for its enzymatic function. Casein kinase 2-mediated S120 phosphorylation negatively regulates NDPK-A enzymatic activity that prevents its autophosphorylation. Thus, NDPK-A enzymatic activity is normally under stringent control by phosphorylation events. NDPK-A is also regulated by redox modification when in an oligomeric state (27). On the other hand, factors that impact the cellular abundance of NDPK-A have not been studied. This mode of regulatory control could interact with phosphorylation or redox modification of the kinase to potentially modulate transferase activity, tumor suppressor function, or kinase effects on signaling.

In this study, we demonstrate that a relatively new F-box protein, FBXO24, mediates NDPK-A ubiquitylation and proteasomal degradation. FBXO24 recruitment to NDPK-A requires two residues, L55 and K56, forming an (I/L)K binding motif. Unexpectedly, GCN5-mediated K56 acetylation (acetyl-K) impairs FBXO24 recruitment to NDPK-A which stabilizes the kinase. Our data support a model whereby an I/L(acetyl-K) motif within NDPK-A displays structural similarities to the F-box recognition motif (I/L)Q, but this serves as a distinct inhibitory molecular signature for FBXO24 recruitment to limit substrate degradation.

MATERIALS AND METHODS

Cells and reagents. HeLa cells were cultured in Eagles minimal essential medium (EMEM) containing 10% of fetal bovine serum (FBS) at 37°C in the presence of 5% CO_2. HEK293 cells were maintained with EMEM supplemented with 10% of FBS at 37°C in the presence of 5% CO_2. Hemagglutinin (HA) tag (catalog no. 2367), ubiquitin (catalog no. 3936), and acetylated-lysine (catalog no. 9441) antibodies were from Cell Signaling (Danvers, MA). Antibodies of NDPK-A (nm23-H1; catalog no. sc-465), FBXO24 (catalog no. sc-138272), and GCN5 (catalog no. sc-20698) were from Santa Cruz Biotechnology (Santa Cruz, CA). V5 tag antibody, pCDNA3.1D-His-V5-TOPO plasmid, and TOP10 competent cells were from Invitrogen (Carlsbad, CA). QuikChange II XL site-directed mutagenesis kits were from Agilent Technologies (Santa Clara, CA). TNT coupled reticulocyte lysate system kits were from Promega (Madison, WI). MLN4924, a cullin-RING ligase inhibitor, was from Cayman Chemical (Ann Arbor, MI). The AMPK activator AIACR was from Sigma-Aldrich (St. Louis, MO).

Construction of plasmids. The open reading frame of the human nucleoside diphosphate kinase A (NDPK-A) was amplified by PCR using the forward primer 5′-CACCATGGCCAACTGTGAGCGTAC-3′ and the reverse primer 5′-GATCCAGTTCTGAGCACAG-3′. The resulting PCR product was purified from an agarose gel, followed by cloning into a pCDNA3.1D-V5-His plasmid. The NDPK-A series deletion mutants were constructed using the following primers: F1, 5′-CACCATGGCCAACTGTGAGCGTAC-3′; F20, 5′-CACCATGCTTGTGGGAGAGATTATCAAG-3′; F40, 5′-CACCATGTTCATGCAAGCTTCCGAAG-3′; F60, 5′-CACCATGTTCTTTGCCGGCCTGGTG-3′; R80, 5′-CCCCTCCCAGACCATGGCAAC-3′; R100, 5′-CTTGGAGTCTGCAGGGTTG-3′; R120, 5′-ACTGCCATGTATAATGTTCCTG-3′; and R150, 5′-GATCCAGTTCTGAGCACAG-3′. The accuracy of the cloned genes was verified by DNA sequencing.

Site-directed mutagenesis. Mutagenesis was introduced by using a QuikChange II XL site-directed mutagenesis kit according to the manufacturer's instruction. Primers for K85, K12, and K56 mutants of NDPK-A were as follows: K85A forward, 5′-GAGGGGCTGAATGTGGTGCGACGGGCCGAGTCATG-3′; K85A reverse, 5′-CATGACTCGGCCCGTCGCCACCACATTCAGCCCCTC-3′; K12A forward, 5′-GTACCTTCATTGCGATCGCACCAGATGGGGTCCAG-3′; K12A reverse, 5′-CTGGACCCCATCTGGTGCGATCGCAATGAAGGTAC-3′; K56R forward, 5′-CAAGCTTCCGAAGATCTTCTCGCGGAACACTACGTTGACCTTGAAG-3′; K56R reverse, 5′-CTTCGGTCAACGTAGTGTTCCGCGAGAAGATCTTCGGAAGCTTG-3′; K56Q forward, 5′-GAACACTACGTTGACCTGCAGGACCGTCCATTCTTTG-3′; and K56Q reverse, 5′-CAAAGAATGGACGGTCCTGCAGGTCAACGTAGTGTTC-3′.

Plasmid transfection. Plasmids were introduced into HeLa cells using TurboFect transfection reagent (Thermo Scientific) according to the manufacturer's instructions. Briefly, cells were inoculated into six-well plates with 2 ml of EMEM containing 10% FBS at 24 h prior to transfection. Transfection was performed when cells reached 70% confluence. The plasmid DNA (3 μg) was mixed with 200 μl of EMEM, followed by the addition of 6 μl of TurboFect reagent. The mixtures were incubated at room temperature for 15 min before they were added to the cells.

Immunoblotting and IP. Immunoblotting and immunoprecipitation (IP) analyses were performed as described previously (28, 29). Cells were harvested and collected with cell lysis buffer (150 mM NaCl, 50 mM Tris-HCl, 1 mM EDTA, 2 mM dithiothreitol [DTT], 0.3% Triton X-100 [vol/vol], and 1:1,000 protease inhibitor mixture). For immunoprecipitation, equal amounts of cell lysates were incubated with specific primary antibodies overnight at 4°C; 35 μl of protein A/G-agarose beads was added to the mixtures and incubated for 2 h at 4°C. The immunoprecipitates were washed three times with cell lysis buffer. The precipitates were mixed with protein sample buffer (50 μl), heated at 70°C for 8 min, and separated on 4 to 12% SDS-PAGE gels (Invitrogen). For each immunoprecipitation study, we loaded 2% of the input as a control and used 50% of the total immunoprecipitates in each IP lane. The separated proteins were transferred onto nitrocellulose membranes and blocked with 5% milk in TTBS buffer (50 mM Tris, 150 mM NaCl, 1% [vol/vol] Tween 20, pH 8.0) for 1 h. The membrane was then incubated with NDPK-A antibody (1:1,000) overnight in TTBS buffer in the presence of 1% milk. Membranes were washed with TTBS buffer three times, for 5 min each time. Membranes were then incubated with secondary antibody (1:2,000) for another 1 h in TTBS buffer with 5% milk. The membrane was again washed with TTBS buffer three times, for 5 min each time. Prior to visualization using a Kodak Streamcare detection system, membranes were incubated with 1 ml of SuperSignal West Femto maximum sensitivity substrate (Thermo Scientific) for 20 s. For β-actin immunoblotting, the concentrations of the first antibody and second antibody were 1:5,000 and 1:2,500, respectively. The signals were visualized with SuperSignal West Pico chemiluminescent substrate (Thermo Scientific).

***In vitro* binding assays.** To identify the FBXO24 binding domain within NDPK-A, we conducted *in vitro* binding assays. V5-tagged NDPK-A deletion mutant proteins were *in vitro* expressed using a TNT coupled reticulocyte lysate system. Endogenous FBXO24 protein was obtained by immunoprecipitation from HeLa cell lysate (1 mg of protein) using FBXO24 antibody and protein A/G-agarose beads (Thermo Scientific). FBXO24-precipitated beads were incubated with a variety of NDPK-A truncations for 2 h, followed by extensive washing. FBXO24-interacting proteins were detected by immunoblotting using anti-V5 antibody (30). NH_2-terminal biotinylated wild-type (WT) and mutant NDPK-A peptides for FBXO24 binding assays were synthesized by LifeTein (Plainfield, NJ). Carboxyl-terminal V5-tagged FBXO24 was *in vitro* expressed using a TNT coupled reticulocyte lysate system generating approximately 300 ng per reaction. The recombinant FBXO24 (~300 ng)

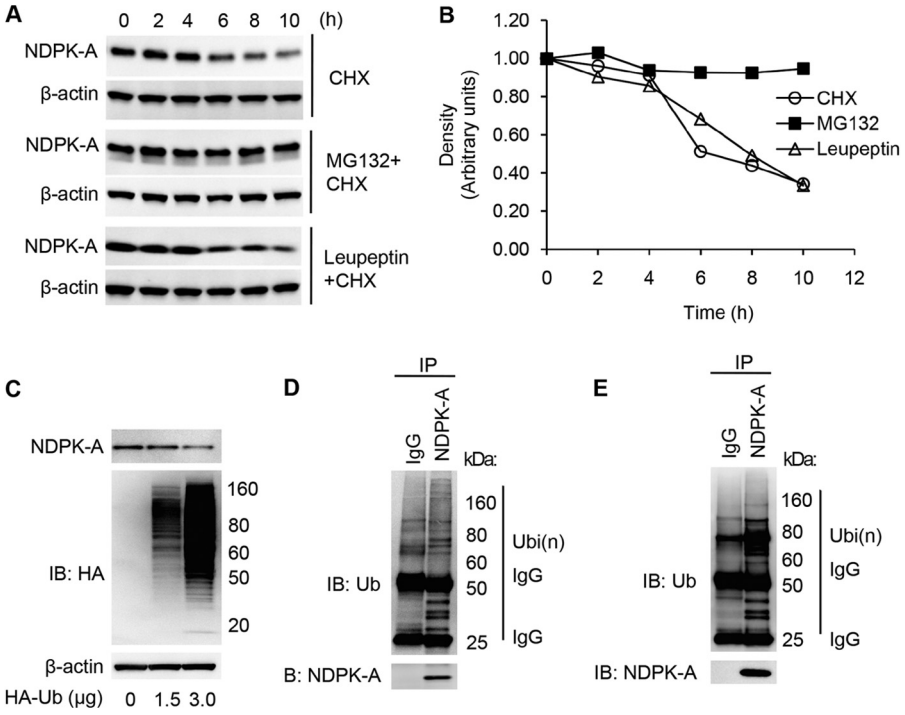

FIG 1 NDPK-A is degraded via the ubiquitin proteasome. (A) Immunoblotting showing NDPK-A degradation in HeLa cells treated with cycloheximide (CHX), CHX in combination with MG132 or leupeptin. β-Actin was used as loading control. (B) Densitometry of results of the experiment shown in panel A. (C) Ectopically expressed HA-ubiquitin plasmid triggers NDPK-A degradation. The immunoblot shows endogenous levels of NDPK-A and levels of hemagglutinin-tagged proteins (HA) and β-actin in lysates of HeLa cells after transfection with different concentrations of plasmids encoding HA-ubiquitin (Ub). (D) NDPK-A is polyubiquitinated in HeLa cells. Immunoprecipitation was performed with primary NDPK-A antibody or IgG in HeLa cell lysates, followed by immunoblotting with ubiquitin antibody. (E) NDPK-A is polyubiquitinated in HEK293 cells. Immunoprecipitation was performed with primary NDPK-A antibody or IgG in cell lysates, followed by immunoblotting with ubiquitin antibody. For panels A and B, there were 3 separate experiments, for panel C, there were 2, and for panels D and E, there was 1 experiment. IB, immunoblotting; Ubi(n), polyubiquitin species.

was mixed with peptides (2 μg) in 0.5 ml of binding buffer (150 mM NaCl, 50 mM Tris-HCl, 0.3% [vol/vol] Tween 20, and 1:1,000 protease inhibitor mixture, pH 7.4) for 2 h at room temperature. Streptavidin beads (40 μl) were added into the mixture for binding for 1 h. The beads were subsequently washed with the binding buffer three times and analyzed by V5 immunoblotting.

Cell migration assays. HeLa cells were grown to 90% confluence in six-well culture plates that were scratched using a pipette tip to produce the wound. The cells were then transfected with a plasmid encoding NDPK-A WT (NDPK-A WT plasmid) or a K85A or K12A mutant protein (K85A or K12A plasmid, respectively). After 24 h of culture, the wound healing was visualized under light microscopy, and the recovered area was calculated using ImageJ software (31, 32). HeLa cell migration was also evaluated using a Transwell migration kit from Trevigrn (Gaithersburg, MD) as described previously (33, 34). Briefly, 50 μl of HeLa cells that had been transfected with plasmid was added to the top chamber, and 150 μl of EMEM containing 10% FBS was added to the lower chamber. After 24 h of culture, the cells that had migrated inside the chamber were dissociated with cell dissociation/calcein-acetoxymethyl (calcein-AM) ester, and the degree of cell migration was determined using a fluorescence microplate reader with 485-nm excitation and 520-nm emission wavelengths (35).

Statistical analysis. All results were analyzed by two-way analysis of variance and a Student *t* test. Data are presented as means ± standard deviations (SD) from three independent experiments.

RESULTS

NDPK-A is degraded via ubiquitin proteasomal processing. To investigate the stability of NDPK-A, HeLa cells were treated with the protein biosynthesis inhibitor cycloheximide (CHX), and the cell lysates were analyzed using immunoblotting. Endogenous NDPK-A decreased in a time-dependent manner (Fig. 1A, top panel), indicating that immunoreactive NDPK-A has a half-life ($t_{1/2}$) of ~6 h in HeLa cells. To understand which pathway is involved in the degradation of NDPK-A, cells were treated with the proteasome inhibitor MG132 (Fig. 1A, middle panel) or the lysosome inhibitor leupeptin (Fig. 1A, bottom panel) in the presence of CHX. MG132 treatment effectively inhibited the degradation of NDPK-A (Fig. 1A and B), suggesting that the kinase is degraded via the ubiquitin proteasomal pathway. In contrast, leupeptin treatment did not impair NDPK-A degradation. To determine if ubiquitylation sufficiently alters NDPK-A stability, we overexpressed hemagglutinin (HA)-tagged ubiquitin in cells and observed that ubiquitin promoted the degradation of NDPK-A in a concentration-dependent manner (Fig. 1C). To verify that NDPK-A is modified by ubiquitylation, we treated cells with MG132 and performed immunoprecipitation with NDPK-A antibody. Analysis of the precipitates by ubiquitin immunoblotting showed that endogenous NDPK-A was polyubiquitinated (Fig. 1D). Similar results were observed in HEK293 cell lines (Fig. 1E). These data demonstrate that NDPK-A protein has an extended life span and that it is degraded via the ubiquitin proteasomal machinery.

FBXO24 mediates the degradation of NDPK-A. NDPK-A is extensively regulated by reversible phosphorylation. Therefore,

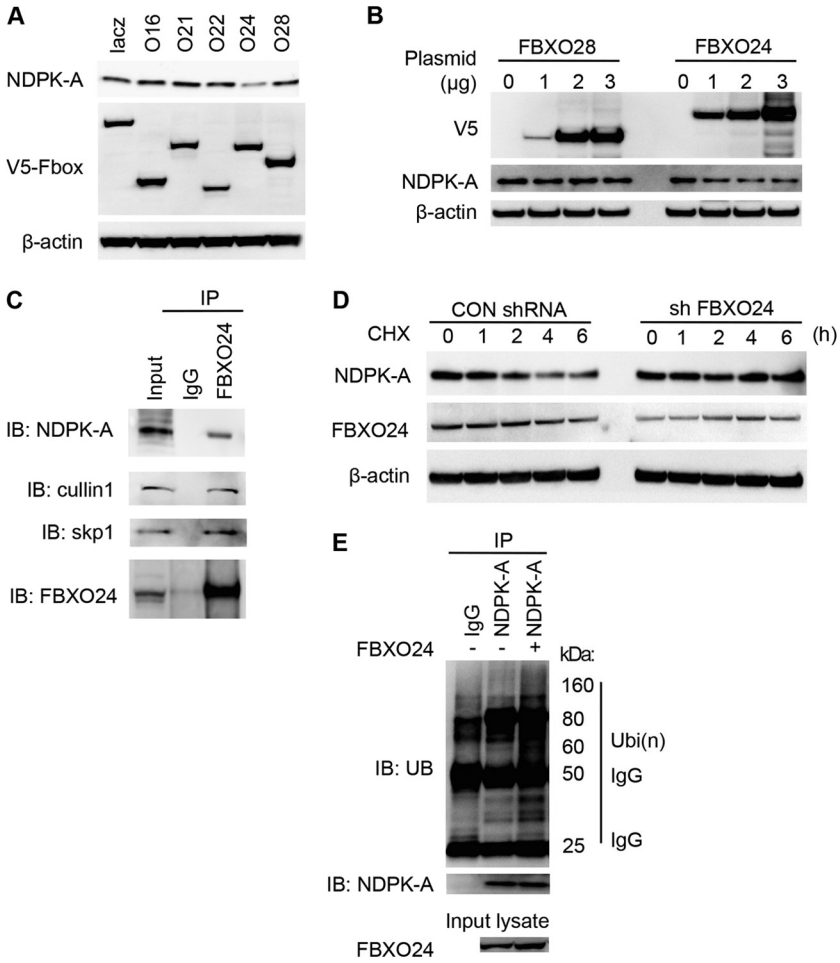

FIG 2 FBXO24 induces the degradation of NDPK-A. (A) Plasmids encoding LacZ or one of several F-box proteins (where O16 is FBXO16, e.g.) were introduced into HeLa cells by transfection. Cell lysates were subjected to immunoblotting with NDPK-A, V5, or β-actin antibodies. (B) Various amounts of V5-FBXO28 or V5-FBXO24 plasmid were introduced into HeLa cells, as indicated. Cell lysates were subjected to immunoblotting to detect endogenous NDPK-A or β-actin levels. (C) SCF-FBXO24 binds NDPK-A. Immunoprecipitation using cell lysates was carried out using FBXO24 primary antibody or IgG, and the precipitates were immunoblotted using NDPK-A, cullin 1, Skp1, or FBXO24 antibodies. (D) FBXO24 knockdown stabilizes NDPK-A from degradation. NDPK-A half-life was determined in cells treated with an shRNA targeting FBXO24 (sh FBXO24) or a scrambled RNA (control, CON). (E) FBXO24 overexpression induces NDPK-A polyubiquitination. NDPK-A ubiquitination was determined in FBXO24 plasmid-overexpressing or control plasmid-treated cells. Cell lysates were subjected to NDPK-A immunoprecipitation, and the precipitates or lysates were analyzed by ubiquitin or FBXO24 immunoblotting. For each panel, there were 3 separate experiments.

we screened potential E3 ubiquitin ligase subunits (F-box proteins), focusing on the SCF family because these components typically target phosphoproteins for their ubiquitylation. We first overexpressed plasmids encoding F-box proteins in cells and assessed NDPK-A stability. Among F-box proteins tested, overexpression of a plasmid encoding FBXO24 (FBXO24 plasmid) selectively led to low abundance of NDPK-A (Fig. 2A). Further, NDPK-A degradation in the FBXO24-overexpressing cells occurred in a concentration-dependent manner (Fig. 2B, right panel). As a control, overexpression of the FBXO28 plasmid did not trigger NDPK-A degradation (Fig. 2B, left panel). Because an E3 ubiquitin ligase component can directly associate with its substrate, we conducted FBXO24 immunoprecipitation followed by NDPK-A immunoblotting of the precipitates. NDPK-A immunoblots showed that FBXO24 associates with NDPK-A, cullin 1, and Skp1 (Fig. 2C). In addition, knockdown of FBXO24 by a specific short hairpin RNA (shRNA) increased NDPK-A stability compared to that with the scrambled RNA control (Fig. 2D). Interestingly, despite only modest knockdown of FBXO24 in these studies, it was sufficient to more robustly lead to accumulation of NDPK-A protein levels in cells. Last, we observed that FBXO24 overexpression increases NDPK-A ubiquitination (Fig. 2E). These results demonstrate that the SCF E3 ubiquitin ligase component FBXO24 interacts with NDPK-A to mediate NDPK-A disposal in cells.

K85 is an NDPK-A ubiquitylation acceptor site. E3 ubiquitin ligases catalyze protein ubiquitylation by covalent ligation of a ubiquitin moiety to an ε-amino group of a lysine residue within the substrate. To investigate which lysine is an acceptor site for ubiquitylation within NDPK-A, we first constructed a series of plasmids encoding NDPK-A truncation mutants (Fig. 3A). We overexpressed the V5-tagged mutants and then treated the cells with MG132. Immunoblotting showed that deletion of the first 80 residues within the carboxyl terminus of NDPK-A remarkably

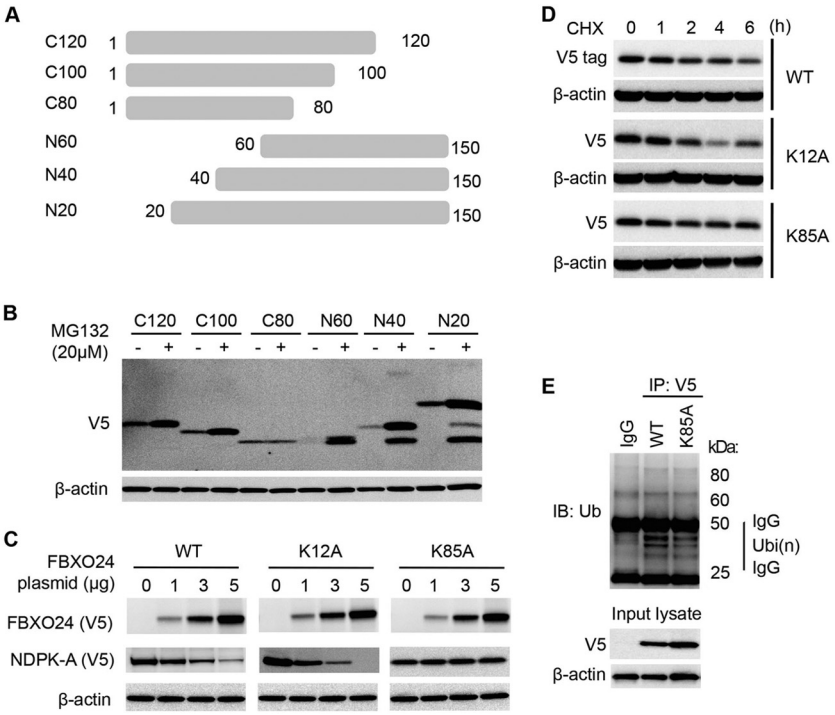

FIG 3 K85 is the ubiquitylation acceptor within NDPK-A. (A) Schematic presentation of NDPK-A deletion mutants. C, C terminus; N, N terminus. (B) Plasmids encoding V5-NDPK-A deletion mutants were overexpressed in HeLa cells for 24 h, and cells were treated with MG132 for 4 h prior to V5 or β-actin immunoblotting. (C) Cells were cotransfected with plasmids encoding the wild-type (WT), K12A, or K85A NDPK-A variant together with an FBXO24 plasmid in HeLa cells for 48 h. The cell lysates were analyzed by V5, FBXO24, or β-actin immunoblotting. (D) V5-tagged plasmids described in panel C were also expressed separately in cells and assayed for degradation in the presence of CHX over time. (E) A V5-NDPK-A WT or K85A mutant plasmid was expressed in cells for 48 h, and cell lysates were used for V5 immunoprecipitation. The immunoprecipitates were immunoblotted with ubiquitin antibody. V5 and β-actin immunoblotting of cell lysates was used as input. For each panel, there were 3 separate experiments.

reduced its accumulation compared to that of the wild type (WT) and other NDPK-A mutants (Fig. 3B). This result suggests that the ubiquitylation site may reside in the region spanning amino acids (aa) 80 to 100. Of note, additional bands were detected on immunoblots after plasmids encoding N-terminal 40- and 20-aa deletion variants (N40 and N20, respectively) were expressed in cells treated with MG132. The observation that these bands are present when MG132 is included in the culture medium suggests that these products arise from proteolytic cleavage or accumulate as misfolded constructs that are normally removed in the cells by the proteasome. Nevertheless, analysis of the primary sequence of this 80- to 100-aa region reveals only one lysine residue at K85. Replacing the K85 residue with an alanine within NDPK-A by site-directed mutagenesis was performed, and the resultant K85A mutant plasmid and WT plasmid were expressed in cells to determine their degradation profiles. Because we observed that NDPK-A degradation was FBXO24 dependent, we examined the degradation patterns of expressed WT, K12A, and K85A mutant proteins after FBXO24 plasmid expression. Immunoblotting results indicated that WT NDPK-A and the K12A mutant protein degrade comparably, but a K85A mutant is more stable under conditions of increased concentrations of FBXO24 expression (Fig. 3C). To confirm this observation, we observed the degradation of the mutants in the presence of CHX. Immunoblotting results showed that the K12A mutant protein degrades at a rate similar to that of the WT protein, but the K85A mutant is more stable than the WT and K12A mutant proteins (Fig. 3D). Further, *in vitro* ubiquitylation studies indicate that the K85A mutant is less ubiquitylated than WT NDPK-A (Fig. 3E). These results suggest that K85 is one likely FBXO24-dependent ubiquitin acceptor site within NDPK-A.

FBXO24 docks on an LK motif within NDPK-A. Since FBXO24 induces the degradation of NDPK-A by its interaction, we next examined the molecular signature within NDPK-A that mediates FBXO24 interaction using an *in vitro* binding assay. A variety of truncated mutants of recombinant mutant proteins (Fig. 4A) were produced by *in vitro* synthesis. Endogenous FBXO24 protein was immunoprecipitated from cell lysates using FBXO24 antibody. The endogenous FBXO24 was mixed with the recombinant mutant proteins, and the precipitates were analyzed by immunoblotting. *In vitro* binding assay results suggested that various deletion constructs lacking the carboxyl terminus of NDPK-A do not result in loss of FBXO24 binding when corrected for loading (Fig. 4B, top blot and input). Notably, unlike WT NDPK-A and a variant lacking the first 40 residues within NDPK-A, the capacity of an NH_2-terminal deletion construct lacking the first 60 aa within the kinase to bind to FBXO24 was substantially reduced to very low levels (Fig. 4B). This suggests that aa 40 to 60 within NDPK-A are required for FBXO24 binding. Further, to fine-map the FBXO24 docking site, we constructed a series of deletion mutants in which we progressively deleted 2 residues from each construct (Fig. 4C and D). Results from the FBXO24 binding assays indicate that residues L55 and K56 within NDPK-A are critical for FBXO24 binding (Fig. 4D). Thus, an

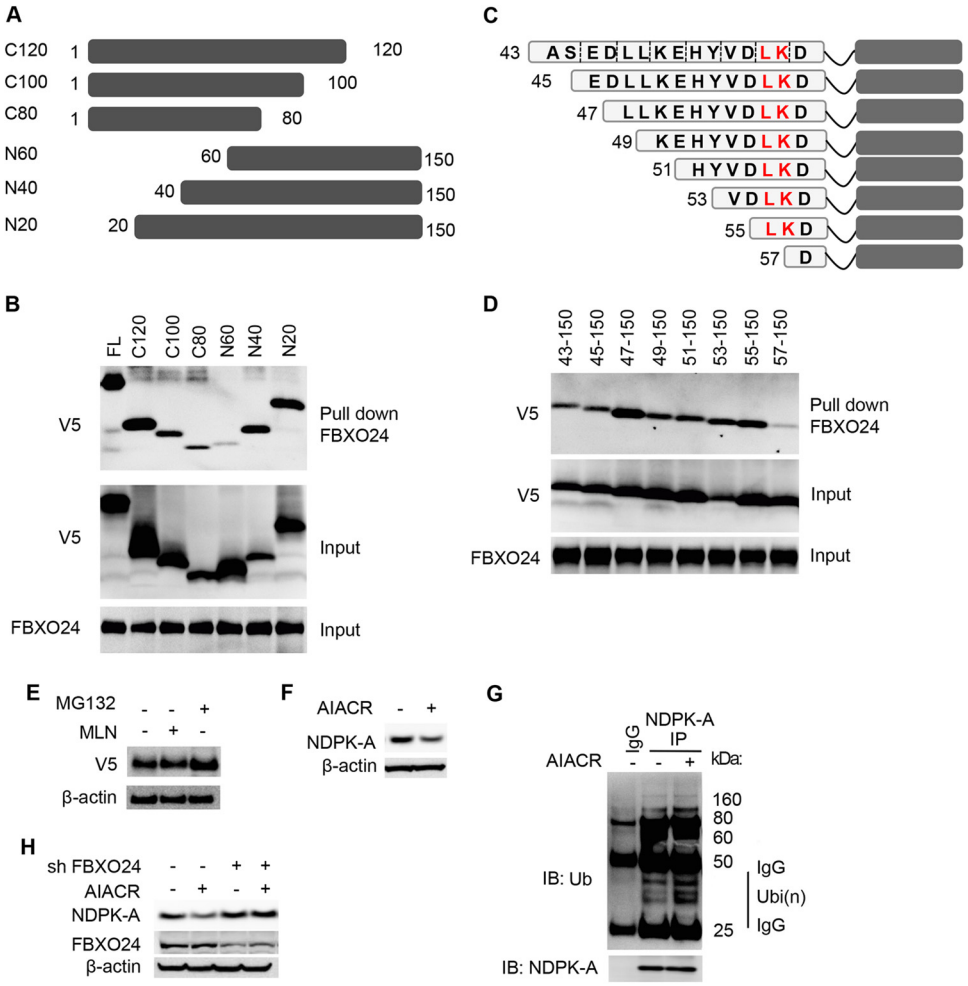

FIG 4 L55 and K56 within NDPK-A are required for FBXO24 interaction. (A) Schematic presentation of NDPK-A deletion mutants. (B) Residues 40 to 60 within NDPK-A are critical for FBXO24 binding. *In vitro* binding assays were performed after *in vitro* translation of NDPK-A truncated proteins and pulldown using FBXO24 beads. The precipitates were analyzed with V5 immunoblotting (top panel). Various truncations of NDPK-A were *in vitro* synthesized (middle panel), and FBXO24 was obtained by immunoprecipitation (bottom panel). FL, full-length. (C and D) Mapping of NDPK-A identifies that L55 and K56 are critical for FBXO24 binding. The amino acids were progressively deleted by 2 residues (C). *In vitro* binding assays were conducted and analyzed by V5 immunoblotting (D). The input was performed as described above. (E) An N60 NDPK-A deletion mutant was expressed in the cells for 24 h; cells were treated with MLN4924 (MLN) or MG132 for 4 h separately. Cell lysates were analyzed by V5 and β-actin immunoblotting. (F) Activation of AMPK reduces NDPK-A protein levels in HEK293 cells. HEK293 cells were treated with the AMPK activator AIACR (500 μM) for 48 h, followed by NDPK-A immunoblot analysis. (G) AMPK activation augments ubiquitination of NDPK-A. Ubiquitination (Ub) levels of NDPK-A were determined in the presence or absence of AIACR (500 μM) in HEK293 cells as described in the legend of Fig. 3E. (H) AMPK-mediated NDPK-A protein reduction is FBXO24 dependent. FBXO24 proteins were depleted by shRNA in HEK293 cells in the presence or absence of AIACR (500 μM). Cell lysates were analyzed by immunoblotting, as indicated. For each panel, there were 3 separate experiments.

(I/L)K motif similar to an (I/L)Q motif recognized by other F-box proteins within NDPK-A is important for FBXO24 docking (10). However, these results do not exclude the contribution from surrounding or adjacent amino acids or structural features of NDPK-A that may partake in FBXO24 binding. Interestingly, in previous experiments we showed that MG132 treatment accumulates the N60 deletion mutant, suggesting that it harbors a ubiquitination acceptor site (Fig. 3B); yet in our binding studies, this variant cannot interact with FBXO24, raising the possibility that another E3 ligase binds and polyubiquitinates NDPK-A (Fig. 4D). To test this hypothesis, we treated cells with MLN4924, a cullin-RING ligase inhibitor, after cellular expression of the N60 construct. Addition of MLN4924 does not change the protein levels of N60 compared with those of the wild type, suggesting that the truncated form of NDPK-A may be degraded by an E3 apparatus other than cullin-RING-based ubiquitin E3 ligases (Fig. 4E). We also assessed the physiologic context of NDPK-A degradation. As AMPK represses activity of NDPK-A (24–26), we first measured steady-state immunoreactive levels of NDPK-A after addition of the AMPK activator AIACR (500 μM). AIACR reduces NDPK-A protein levels in HEK293 cells (Fig. 4F) and increases the ubiquitination of NDPK-A (Fig. 4G), and the AIACR reduction of immunoreactive levels of NDPK-A can be rescued by depletion of FBXO24 (Fig. 4H). These data suggest that AMPK inhibits NDPK-A activity by reducing NDPK-A protein levels through ubiquitin-proteasomal degradation.

Acetylation of K56 of the LK motif regulates NDPK-A stability. Lysine residues within proteins are also susceptible to post-translational modification by acetylation (36). Protein acetylation also competes with ubiquitylation at molecular sites. Indeed, en-

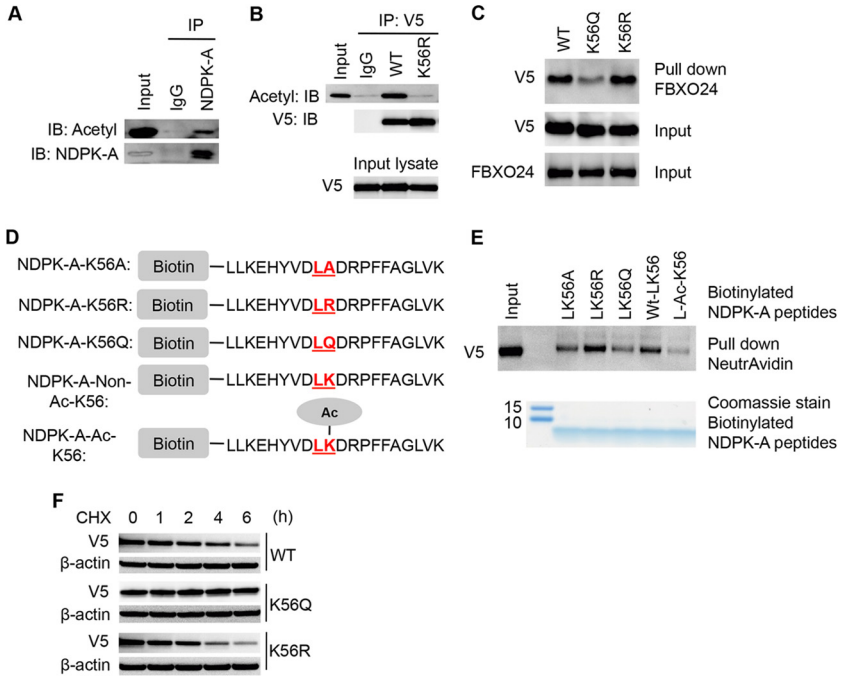

FIG 5 K56 is an acetylation site within NDPK-A that regulates FBXO24 binding. (A) Endogenous NDPK-A was immunoprecipitated from HeLa cell lysates and subjected to acetyllysine immunoblotting. (B) A WT or K56R mutant NDPK-A plasmid was expressed in HeLa cells. The cell lysates were subjected to V5 immunoprecipitation, and the precipitates were immunoblotted with acetyllysine antibody. (C) Acetylation of K56 within NDPK-A reduces its binding to FBXO24. WT, K56Q (an acetylation mimic, NDPK-A-Ac-K56), and K56R (nonacetylation mimic, NDPK-A-Non-Ac-K56) NDPK-A plasmids were expressed in HeLa cells. Cell lysates were processed for FBXO24 pulldown or V5 or FBXO24 immunoblotting, as indicated. (D) NDPK-A peptide binding to FBXO24. Biotinylated 20-aa fragments of NDPK-A spanning the L55-K56 region were used in pulldown assays. (E) Fragments harboring mutations at K56 or containing acetylated K56 (Ac-LK56) or nonacetylated K56 (Wt-LK56) were used in direct binding assays with FBXO24. After incubation with peptides and FBXO24, the biotinylated samples were washed extensively and pulled down using NeutrAvidin. The relative binding to V5-FBXO24 was visualized using V5 immunoblotting. The bottom panel shows Coomassie staining to control for loading with biotinylated NDPK-A peptides. (F) Half-life of NDPK-A mutants. Cells transfected with a WT, K56Q, or K56R plasmid were exposed to CHX and processed for degradation over time. For each panel, there were 3 separate experiments.

dogenous NDPK-A is acetylated, as shown by coimmunoprecipitation (Fig. 5A). We next assessed if NDPK-A K56 is an acetylation site by V5 immunoprecipitation followed by acetyllysine immunoblotting. Compared to WT NDPK-A acetylation levels, unexpectedly the K56R mutant showed reduced levels of acetylation, suggesting that K56 is a major acetylation site within NDPK-A as well as an FBXO24 binding residue (Fig. 5B). To understand the role of K56 acetylation within NDPK-A, we tested its impact on interaction with FBXO24. K56 was replaced by either a glutamine (Q) to mimic an acetylated lysine or an arginine (R) to mimic a nonacetylation residue that retains similar charge properties to engage FBXO24. As shown in an *in vitro* binding assay, the K56Q mutant showed reduced interaction with FBXO24 compared to the wild-type NDPK-A. In addition, the K56R mutant exhibited somewhat increased interaction with FBXO24 (Fig. 5C). These results suggest that K56 acetylation within NDPK-A impairs binding to FBXO24. To verify these results, we tested biotinylated NDPK-A peptides (20 aa) that had intact L55 residues but harbored various amino acid substitutions at K56 to assess their binding to FBXO24 in pulldown studies. In addition, we examined the ability of a K56-acetylated peptide to interact with the F-box protein (Fig. 5D). Consistent with the results shown in Fig. 5C, a K56R peptidic fragment exhibited high-level binding to FBXO24, whereas nonacetylated K56 and K56A peptides retained the ability to engage the F-box protein (Fig. 5E). A K56Q peptide showed reduced binding compared to other peptides, whereas an acetylated K56 peptide showed limited FBXO24 interaction (Fig. 5E). These *in vitro* studies provide more direct evidence of the role of NDPK-A acetylation and its interaction with SCF-FBXO24. Last, we observed the degradation of NDPK-A mutants in the presence of CHX. Consistent with the above observations, expression of a K56Q NDPK-A mutant protein in cells resulted in an extended half-life, whereas a K56R mutant degraded rapidly compared to the WT NDPK-A because it retained electrostatic properties sufficient to mediate interaction with FBXO24 (Fig. 5F). Thus, K56 is essential for FBXO24 interaction, and the data suggest that the ability of this molecular site to mediate binding with the F-box protein is impaired when K56 is acetylated, which is a posttranslational modification critical for conferring NDPK-A stability. Last, the ability of WT NDPK-A to be acetylated and yet retain the ability to bind FBXO24 suggests that there may be other acceptor sites for acetylation within the kinase that do not impact FBXO24 association (Fig. 4A and 5B).

GCN5 acetylates NDPK-A to regulate its degradation. Given the fact that the acetylation status at K56 impairs the NDPK-A binding capacity to FBXO24, we attempted to identify the acetyltransferase(s) that modifies K56 within NDPK-A. Thus, we conducted immunoprecipitation with an NDPK-A antibody, followed by immunoblotting analysis. Among the acetyltransferases tested (data not shown), we found that GCN5 interacted with NDPK-A (Fig. 6A). Cells were next transfected with GCN5 plasmid or an shRNA targeting GCN5 (GCN5 shRNA) to modulate

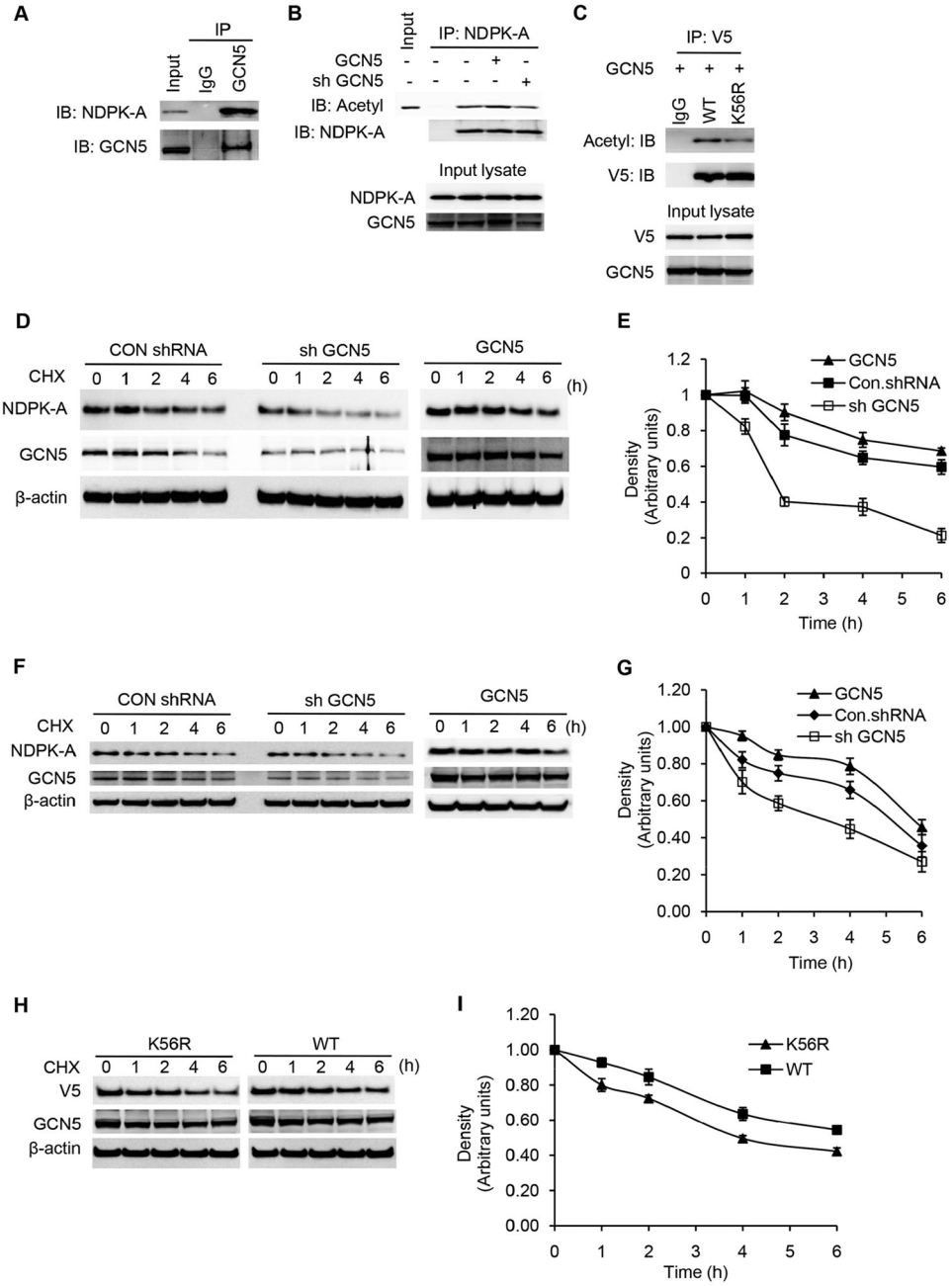

FIG 6 GCN5 regulates NDPK-A acetylation. (A) GCN5 interacts with NDPK-A. Immunoprecipitation of GCN5 was performed in cells, and the precipitates were analyzed by NDPK-A or GCN5 immunoblotting. (B) NDPK-A acetylation is regulated by GCN5. Cells were ectopically expressed with GCN5 plasmid or an shRNA targeting GCN5. Lysates were subjected to NDPK-A IP, followed by immunoblotting with antibody to acetyllysine (Acetyl) or NDPK-A. The lower blots show inputs probed for NDPK-A or GCN5. (C). Acetylation of K56 within NDPK-A by GCN5. A plasmid encoding GCN5 together with either a V5-WT or V5-K56R mutant NDPK-A plasmid was introduced into cells, and cell lysates were subjected to V5 immunoprecipitation. The precipitates were immunoblotted with acetyllysine, GCN5, or V5 antibody as indicated. (D) Regulation of NDPK-A protein abundance by GCN5. GCN5 was knocked down by specific shRNA or overexpressed in HeLa cells during a CHX exposure time course; the cell lysates were analyzed with NDPK-A, GCN5, or β-actin by immunoblotting. (E) The densitometry results of panel D were plotted. (F) GCN5 regulates NDPK-A ubiquitin proteasomal degradation in HEK293 cells. GCN5 was knocked down or overexpressed in HEK293 cells as described above; the cell lysates were used in immunoblotting and analyzed for NDPK-A, GCN5, or β-actin. (G) The densitometry results of panel F were plotted. (H) Overexpression of GCN5 does not stabilize an NDPK-A K56R mutant from degradation. A wild-type or K56R NDPK-A plasmid was coexpressed with GCN5 in HeLa cells for 48 h. The half-lives of wild-type and K56R NDPK-A proteins were analyzed. (I) The densitometry results of panel H were plotted. For each panel, there were 3 separate experiments.

acetyltransferase levels in cells, and then lysates were subjected to NDPK-A immunoprecipitation, followed by immunoblotting with acetyllysine antibodies (Fig. 6B). Ectopically expressed GCN5 plasmid increased NDPK-A acetylation, whereas depletion of GCN5 using shRNA reduced kinase acetylation (Fig. 6B, top blot). To identify the GCN5-mediated acetylation site(s) within NDPK-A, we coexpressed a GCN5 plasmid in cells with either the wild type or a mutant NDPK-A plasmid in which a candidate

lysine residue was mutated. We then conducted immunoprecipitation and analyzed the precipitates with acetyllysine antibody in immunoblotting. The acetylation level of the K56R mutant was reduced compared with that of the WT NDPK-A (Fig. 6C), suggesting that GCN5 acts through this site within NDPK-A. GCN5 depletion in cells by a specific shRNA showed reduced GCN5 at the protein level by ~52%, indicating that the shRNA was partially successful. As expected, NDPK-A degraded more efficiently in cells treated with the GCN5 shRNA than in cells treated with the scrambled RNA control, indicating that GCN5 contributes to the regulation of NDPK-A stability (Fig. 6D). In reciprocal studies, overexpression of *GCN5* in the cells increased GCN5 levels by 150% but only modestly, if at all, stabilized NDPK-A and reduced degradation (Fig. 6D, right panel, and E). These results suggest that the acetyl-acceptor sites may be heavily saturated within NDPK-A, consistent with it being largely acetylated in the native state (Fig. 6A) and sensitive to degradation despite modest depletion of GCN5 (Fig. 6D). We obtained similar results in HEK293 cells (Fig. 6F and G), indicating that GCN5 regulation of NDPK-A ubiquitin proteasomal degradation is not restricted to one cell type. In addition, cocellular expression of GCN5 with the NDPK-A K56R mutant, as a mimic of an unacetylated lysine site that binds to FBXO24, produced an accelerated decay pattern compared to that of the wild-type NDPK-A (Fig. 6H and I). Overall, these data suggest that GCN5 stabilizes NDPK-A via site-specific acetylation.

NDPK-A proteolytically stable mutants inhibit cell migration. One of the functions of NDPK-A is to inhibit metastasis of tumor cells (37). A fundamental characteristic of highly metastatic tumor cells is their ability to display increased cell growth and migration potential. Thus, as a measure of NDPK-A function, we determined if expression of NDPK-A WT and mutant plasmids in cells that exhibit altered protein stability might impact cell migration behavior. We conducted an *in vitro* wound-healing assay and transwell migration assay to address this issue. Here, a linear wound is inflicted initially on the cell monolayer (Fig. 7A, far left). Overexpression of a WT NDPK-A plasmid inhibited cell migration, as reflected by a larger linear wound at 24 h than in untreated (normal control) cells (Fig. 7, NC) or cells transfected with a control vector (LacZ plasmid) (Fig. 7A, CON vector). Notably, forced expression of a ubiquitylation-resistant K85A mutant plasmid significantly repressed cell migration and delayed wound recovery compared with expression of either the WT NDPK-A or the K12A mutant plasmid (Fig. 7A and B). In a Transwell system similar results were observed (Fig. 7C). We conducted shRNA knockdown of FBXO24 in HeLa cells to assess the role of the endogenous F-box protein in cell migration behavior. Wound-healing assays indicated that cell migration was inhibited to a greater extent after 24 h in FBXO24 knockdown cells than in cells treated with a scrambled RNA or nontreated cells (Fig. 7D and E). We also observed similar results in transwell assays (Fig. 7F). Last, we transfected cells with either a WT NDPK-A or control plasmid or cotransfected a WT, K56R, or K56Q mutant NDPK-A plasmid in cells with the FBXO24 plasmid (Fig. 7G). While the control plasmids when expressed triggered nearly complete wound healing, expression of the WT NDPK-A plasmid alone in cells partially impaired wound healing, consistent with its anti-cell migration effect. However, cotransfection in cells of either the WT or K56R NDPK-A plasmid that effectively bind FBXO24 together with the FBXO24 plasmid led to nearly complete closure of the wound. Thus, because FBXO24 degrades both WT and K56R NDPK-A proteins through interactions, this is sufficient to impair cell migration. Finally, cotransfection of FBXO24 with the acetylation mimic NDPK-A plasmid (K56Q) limited wound repair (Fig. 7G and H). As predicted, because the K56Q NDPK-A protein does not effectively interact with FBXO24, the stabilized protein limited cell proliferative behavior. These data indicate that NDPK-A protein stability impacts cell migration.

DISCUSSION

The primary findings in this study are that (i) NDPK-A is a protein that exhibits intermediate stability in cells and is degraded via ubiquitin proteasomal degradation, (ii) NDPK-A stability is attributed, in part, to its site-specific acetylation regulated by GCN5, (iii) the orphan F-box protein, FBXO24, targets NDPK-A for its elimination in cells, and (iv) the molecular signature identified here, (I/L)acetyl-K, hinders the ability of FBXO24 to interact with NDPK-A, thereby protecting the enzyme from degradation. The ability of substrate acetylation to inhibit SCF component interaction provides a unique mechanism whereby the cell may preserve the abundance of a protein to elicit particular functions (Fig. 8). Here, the differential stability of NDPK-A variants when expressed in cells modulated cellular migration, and cellular exposure to an AMPK agonist triggered NDPK-A degradation, an effect reversed by FBXO24 depletion. The data emphasize the role of protein stability as a regulatory mechanism for NDPK-A under some scenarios. As NDPK-A is central in affecting cellular proliferation, the inability of a modified acetyl-K56 kinase to become effectively recognized by the E3 complex could affect other biological functions relating to tumorigenesis, tissue repair, or organogenesis.

Several posttranslational modifications contribute to recruitment of F-box proteins to mediate protein degradation. These posttranslational modifications label or prime proteins destined for ubiquitylation, and this prepares the protein for further processing by the 20S proteasome. Posttranslational modifications such as phosphodegrons can also mask or unmask important molecular signatures that impact the accessibility of the E3 ubiquitin ligase binding motif within a substrate to modulate ubiquitylation and downstream processing (6). Hence, it is not unusual for the phosphorylation site(s) to reside within the binding motif or be juxtaposed to the recognition domain. Glycosylation also controls F-box protein recruitment and substrate binding, and this is especially applicable for FbxO subunits (38). For example, in endoplasmic reticulum (ER) stress-associated degradation, the F-box proteins Fbxo2 and Fbxo6 bind to glycosylated substrates within F-box-associated domains (6). Structural or domain-based recognition factors, as described for telomeric repeat-binding factor 1, may also be important for F-box protein binding within NDPK-A, which requires additional study (39).

The molecular signatures that guide recruitment of F-box protein components to the targeted substrate for ubiquitylation also vary considerably and are stringently controlled (40, 41). The E3 ubiquitin ligase binding motif within substrates could be a stretch of amino acids or the collective effect of a series of low-affinity binding sites or be restricted to one or two amino acid residues (42). Among these motifs, phosphorylation of sites resulting in a phosphodegron such as DSGXXS (X represents any residue) represents a crucial molecular recognition signature for Fbxw1 and Fbxw11. In this motif the serine residues undergo sequential

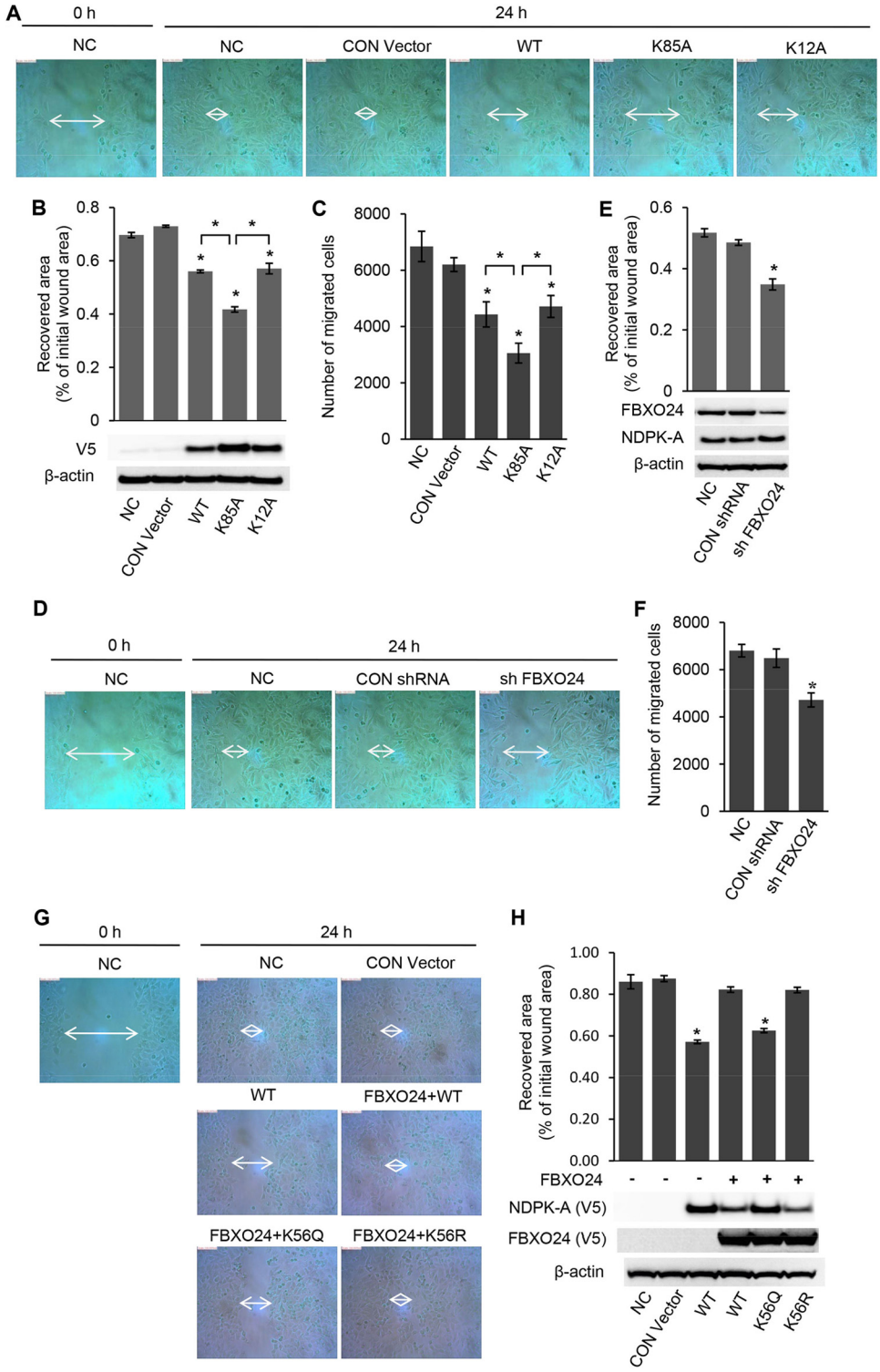

FIG 7 Degradation-resistant NDPK-A inhibits cell migration. (A) HeLa cells (90% confluent in six-well culture plates) were scratched to allow observation of wound repair under normal control (NC) conditions or after transfection with a control (CON; LacZ) vector or NDPK-A WT, K85A, or K12A mutant plasmid for 24 h separately. Wound-healing (arrow) was monitored by the measurement of cell migration distances. (B) Images in panel A were analyzed by ImageJ software for scratch areas. The lower panel shows protein expression levels in cells. (C) Transwell migration assays were performed under control conditions and in cells expressing NDPK-A WT or a K12A, K85A, or LacZ mutant. (D) Knockdown of FBXO24 by shRNA enhances NDPK-A-mediated cell migration inhibition. Wound-healing assays were performed as described for panel A. (E) Images shown in panel D were analyzed by ImageJ software for scratch area. Lower panels show protein expression levels. (F) Transwell migration assays were performed in FBXO24 knockdown cells. (G) Cells were transfected with either WT NDPK-A or a control plasmid or cotransfected with a WT or K56R or K56Q mutant NDPK-A plasmid with FBXO24 plasmid prior to measurement of cell migration distances. (H) Images in panel G were also analyzed by ImageJ software for scratch areas. Lower panels show protein expression levels in cells. In each bar graph, data represent means ± standard errors. *, $P < 0.05$, in each panel for groups indicated versus NC or control vector or between individual groups. For each panel, there were 3 separate experiments.

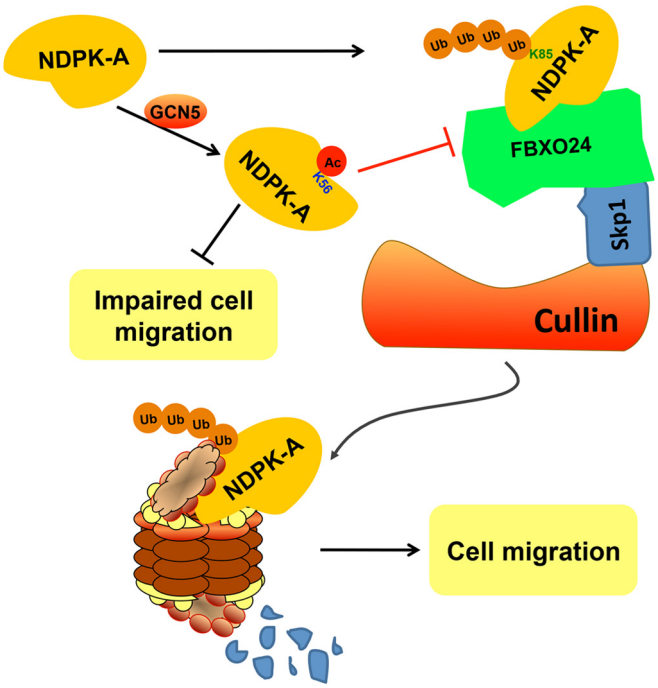

FIG 8 Acetylation stabilizes NDPK-A by opposing SCF-FBXO24 binding. At right, SCF-FBXO24 interacts with NDPK-A to mediate NDPK-A ubiquitylation at K85. At left, GCN5 interacts with NDPK-A to acetylate (Ac) the kinase at K56 within an FBXO24 binding motif, thus serving as an inhibitory molecular mark that impairs recognition by FBXO24. NDPK-A acetylation subsequently stabilizes NDPK-A from SCF-FBXO24-mediated degradation, thereby facilitating the ability of the kinase to impair cell migration.

phosphorylation prior to F-box protein docking on the substrate. Further, while Fbxw7 binds to a proline-enriched signature (TPPXS) (43) and while cyclin F recognizes an RX(I/L) motif (43), some F-box proteins recognize several phosphorylated sites through a successive threshold mechanism that may increase binding affinities for F-box–substrate pairs (44). By using *in vitro* binding assays, we determined that an LK motif within NDPK-A is critical for FBXO24 recruitment to the kinase. This motif somewhat resembles the recognition signatures for some other related FbxL family members as an LQ motif mediates interaction for FbxL2 protein (10). However, FbxL2 also binds to a conserved tryptophan residue within tumor necrosis factor receptor-associated factor (TRAF) adaptor proteins, underscoring variations in binding preferences by an individual F-box protein (30).

These findings showing that acetylation inhibits F-box protein binding were unexpected and raise possibilities for a more complex regulatory model with interactions between acetylation and other posttranslational modifications within NDPK-A. Here, a unique molecular recognition signature, a "deacetyldegron" (LK), promotes FBXO24 recruitment to its target, whereas acetyl-K56 impairs F-box protein binding. Associations between FBXO24 and NDPK-A were demonstrated using modified acetyl-peptides *in vitro* and acetylation mimics and after modulation of GCN5 levels in cells. Because an acetylated lysine residue is structurally similar to glutamine (Q), we pursued the possibility that the presence of an (I/L)K motif could be misread by SCF components as an (I/L)Q binding motif once the lysine residue is modified by acetylation. However, unlike an (I/L)Q motif that promotes FbxL interaction with its target, an acetylated lysine juxtaposed to leucine within NDPK-A represents an inhibitory signal for F-box recruitment. Hence, NDPK-A acetylation may serve as a mechanism to retain catalytic activity by limiting SCF-FBXO24-mediated degradation. Secondary effects by kinase acetylation that induce conformational changes to alter the ability of NDPK-A to associate as oligomeric or hexameric complexes or affect its redox state or interaction with other binding partners could also be regulated. For example, replacing S120 with glycine within NDPK-A destabilizes the protein in the presence of urea, reduces its phosphate-transferase activity, and increases its hexameric state (45). How NDPK-A acetylation coordinates mechanistically to preserve enzyme activity when the kinase is also phosphorylated is unclear and would entail determining the kinetics of K56 acetylation during concomitant phosphorylation at S122 and S144. These modifications would need to be correlated with FBXO24 binding and NDPK-A function. Interestingly, the ability of acetylated NDPK-A to exhibit reduced association with FBXO24 resembles the behavior of the tumor suppressor-like protein Ras association domain family 5 (RASSF5), with its interaction with the HECT family E3 ligase, Itchy E3 ubiquitin protein ligase (Itch). Although no direct evidence was provided, RASSF5 stability was enhanced with reduced binding to Itch in cells after treatment with a deacetylation inhibitor (46). Hence, acetylation may be a more widespread molecular recognition signal among E3 ligases but may function in a capacity to provide exquisite feedback control to extend the cellular protein life span.

The functional relevance of NDPK-A ubiquitination and acetylation was examined in a model of enhanced cellular migration, a key feature of highly metastatic tumors. There is mounting experimental evidence suggesting that NDPK-A impairs tumor progression by inhibiting metastasis. Here, cellular expression of plasmids encoding either a ubiquitylation (K85R)-defective mutant or wild-type NDPK-A blocked cell migration behavior in both a wound-healing assay and a transwell assay. In the context of FBXO24 expression, a plasmid encoding an acetylation (K56Q) NDPK-A mimic that is defective in FBXO24 binding resulted in delayed wound healing compared to expression of plasmids encoding NDPK-A proteins that retain the ability to interact with the F-box protein. FBXO24 depletion in cells also reduced cell migration, suggesting that strategies directed at antagonism of FBXO24 or its binding to NDPK-A or methods to enhance NDPK-A acetylation may also be potential approaches to control tumor metastasis.

ACKNOWLEDGMENTS

This work was supported, in part, by National Institutes of Health R01 grants HL096376, HL097376, HL098174, HL081784, 1UH2HL123502, P01 HL114453 (to R.K.M.) and American Heart Association Award 12SDG12040330 (to C.Z.). This work was also supported in part by the U.S. Department of Veterans Affairs, Veterans Health Administration, Office of Research and Development, Biomedical Laboratory Research and Development, and a Merit Review Award from the U.S. Department of Veterans Affairs. This work was also supported, in part, by grants from the National Project for Significant New Drugs Development of the MOST of China (2012ZX09103-301-033 and 2012ZX09202-301-001), the Natural Science Foundation of China (30873082), and the Major Biotech Industrialization Projects from the Guangzhou Municipal Science and Technology Bureau (2010U1-E00541) to W.C., S.X., and X.L.

REFERENCES

1. **Nalepa G, Rolfe M, Harper JW.** 2006. Drug discovery in the ubiquitin-proteasome system. Nat Rev Drug Discov **5:**596–613. http://dx.doi.org/10.1038/nrd2056.
2. **Gagne JM, Downes BP, Shiu SH, Durski AM, Vierstra RD.** 2002. The F-box subunit of the SCF E3 complex is encoded by a diverse superfamily of genes in *Arabidopsis*. Proc Natl Acad Sci U S A **99:**11519–11524. http://dx.doi.org/10.1073/pnas.162339999.
3. **Skowyra D, Craig KL, Tyers M, Elledge SJ, Harper JW.** 1997. F-box proteins are receptors that recruit phosphorylated substrates to the SCF ubiquitin-ligase complex. Cell **91:**209–219. http://dx.doi.org/10.1016/S0092-8674(00)80403-1.
4. **Winston JT, Koepp DM, Zhu C, Elledge SJ, Harper JW.** 1999. A family of mammalian F-box proteins. Curr Biol **9:**1180–1182. http://dx.doi.org/10.1016/S0960-9822(00)80021-4.
5. **Zheng N, Schulman BA, Song L, Miller JJ, Jeffrey PD, Wang P, Chu C, Koepp DM, Elledge SJ, Pagano M, Conaway RC, Conaway JW, Harper JW, Pavletich NP.** 2002. Structure of the Cul1-Rbx1-Skp1-F box^{Skp2} SCF ubiquitin ligase complex. Nature **416:**703–709. http://dx.doi.org/10.1038/416703a.
6. **Skaar JR, Pagan JK, Pagano M.** 2013. Mechanisms and function of substrate recruitment by F-box proteins. Nat Rev Mol Cell Biol **14:**369–381. http://dx.doi.org/10.1038/nrm3582.
7. **Chowdhury R, McDonough MA, Mecinovic J, Loenarz C, Flashman E, Hewitson KS, Domene C, Schofield CJ.** 2009. Structural basis for binding of hypoxia-inducible factor to the oxygen-sensing prolyl hydroxylases. Structure **17:**981–989. http://dx.doi.org/10.1016/j.str.2009.06.002.
8. **Glenn KA, Nelson RF, Wen HM, Mallinger AJ, Paulson HL.** 2008. Diversity in tissue expression, substrate binding, and SCF complex formation for a lectin family of ubiquitin ligases. J Biol Chem **283:**12717–12729. http://dx.doi.org/10.1074/jbc.M709508200.
9. **Lee JM, Lee JS, Kim H, Kim K, Park H, Kim JY, Lee SH, Kim IS, Kim J, Lee M, Chung CH, Seo SB, Yoon JB, Ko E, Noh DY, Kim KI, Kim KK, Baek SH.** 2012. EZH2 generates a methyl degron that is recognized by the DCAF1/DDB1/CUL4 E3 ubiquitin ligase complex. Mol Cell **48:**572–586. http://dx.doi.org/10.1016/j.molcel.2012.09.004.
10. **Chen BB, Coon TA, Glasser JR, Mallampalli RK.** 2011. Calmodulin antagonizes a calcium-activated SCF ubiquitin E3 ligase subunit, FBXL2, to regulate surfactant homeostasis. Mol Cell Biol **31:**1905–1920. http://dx.doi.org/10.1128/MCB.00723-10.
11. **Chen BB, Glasser JR, Coon TA, Zou C, Miller HL, Fenton M, McDyer JF, Boyiadzis M, Mallampalli RK.** 2012. F box protein FBXL2 targets cyclin D2 for ubiquitination and degradation to inhibit leukemic cell proliferation. Blood **119:**3132–3141. http://dx.doi.org/10.1182/blood-2011-06-358911.
12. **Chen BB, Glasser JR, Coon TA, Mallampalli RK.** 2012. F-box protein FBXL2 exerts human lung tumor suppressor-like activity by ubiquitin-mediated degradation of cyclin D3 resulting in cell cycle arrest. Oncogene **31:**2566–2579. http://dx.doi.org/10.1038/onc.2011.432.
13. **Roymans D, Willems R, Van Blockstaele DR, Slegers H.** 2002. Nucleoside diphosphate kinase (NDPK/NM23) and the waltz with multiple partners: possible consequences in tumor metastasis. Clin Exp Metastasis **19:**465–476. http://dx.doi.org/10.1023/A:1020396722860.
14. **Leone A, Flatow U, King CR, Sandeen MA, Margulies IM, Liotta LA, Steeg PS.** 1991. Reduced tumor incidence, metastatic potential, and cytokine responsiveness of nm23-transfected melanoma cells. Cell **65:**25–35. http://dx.doi.org/10.1016/0092-8674(91)90404-M.
15. **Steeg PS, Cohn KH, Leone A.** 1991. Tumor metastasis and nm23: current concepts. Cancer Cells **3:**257–262.
16. **Otsuki Y, Tanaka M, Yoshii S, Kawazoe N, Nakaya K, Sugimura H.** 2001. Tumor metastasis suppressor nm23H1 regulates Rac1 GTPase by interaction with Tiam1. Proc Natl Acad Sci U S A **98:**4385–4390. http://dx.doi.org/10.1073/pnas.071411598.
17. **Marino N, Marshall JC, Steeg PS.** 2011. Protein-protein interactions: a mechanism regulating the anti-metastatic properties of Nm23-H1. Naunyn-Schmiedeberg's Arch Pharmacol **384:**351–362. http://dx.doi.org/10.1007/s00210-011-0646-6.
18. **Murakami M, Meneses PI, Knight JS, Lan K, Kaul R, Verma SC, Robertson ES.** 2008. Nm23-H1 modulates the activity of the guanine exchange factor Dbl-1. Int J Cancer **123:**500–510. http://dx.doi.org/10.1002/ijc.23568.
19. **Tso PH, Wang YC, Yung LY, Tong Y, Lee MMK, Wong YH.** 2013. RGS19 inhibits Ras signaling through Nm23H1/2-mediated phosphorylation of the kinase suppressor of Ras. Cell Signal **25:**1064–1074. http://dx.doi.org/10.1016/j.cellsig.2013.02.010.
20. **Zhu J, Tseng YH, Kantor JD, Rhodes CJ, Zetter BR, Moyers JS, Kahn CR.** 1999. Interaction of the Ras-related protein associated with diabetes rad and the putative tumor metastasis suppressor NM23 provides a novel mechanism of GTPase regulation. Proc Natl Acad Sci U S A **96:**14911–14918. http://dx.doi.org/10.1073/pnas.96.26.14911.
21. **Iwashita S, Fujii M, Mukai H, Ono Y, Miyamoto M.** 2004. Lbc proto-oncogene product binds to and could be negatively regulated by metastasis suppressor nm23-H2. Biochem Biophys Res Commun **320:**1063–1068. http://dx.doi.org/10.1016/j.bbrc.2004.06.067.
22. **Subramanian C, Cotter MA, II, Robertson ES.** 2001. Epstein-Barr virus nuclear protein EBNA-3C interacts with the human metastatic suppressor Nm23-H1: a molecular link to cancer metastasis. Nat Med **7:**350–355. http://dx.doi.org/10.1038/85499.
23. **Subramanian C, Robertson ES.** 2002. The metastatic suppressor Nm23-H1 interacts with EBNA3C at sequences located between the glutamine- and proline-rich domains and can cooperate in activation of transcription. J Virol **76:**8702–8709. http://dx.doi.org/10.1128/JVI.76.17.8702-8709.2002.
24. **Crawford RM, Treharne KJ, Arnaud-Dabernat S, Daniel JY, Foretz M, Viollet B, Mehta A.** 2006. Understanding the molecular basis of the interaction between NDPK-A and AMPK α1. Mol Cell Biol **26:**5921–5931. http://dx.doi.org/10.1128/MCB.00315-06.
25. **King JD, Jr, Lee J, Riemen CE, Neumann D, Xiong S, Foskett JK, Mehta A, Muimo R, Hallows KR.** 2012. Role of binding and nucleoside diphosphate kinase A in the regulation of the cystic fibrosis transmembrane conductance regulator by AMP-activated protein kinase. J Biol Chem **287:**33389–33400. http://dx.doi.org/10.1074/jbc.M112.396036.
26. **Onyenwoke RU, Forsberg LJ, Liu L, Williams T, Alzate O, Brenman JE.** 2012. AMPK directly inhibits NDPK through a phosphoserine switch to maintain cellular homeostasis. Mol Biol Cell **23:**381–389. http://dx.doi.org/10.1091/mbc.E11-08-0699.
27. **Kim MS, Jeong J, Lee KJ, Shin DH.** 2010. A preliminary X-ray study of human nucleoside diphosphate kinase A under oxidative conditions. Acta Crystallogr Sect F Struct Biol Cryst Commun **66:**1490–1492. http://dx.doi.org/10.1107/S1744309110036067.
28. **Zou C, Butler PL, Coon TA, Smith RM, Hammen G, Zhao Y, Chen BB, Mallampalli RK.** 2011. LPS impairs phospholipid synthesis by triggering β-transducin repeat-containing protein (β-TrCP)-mediated polyubiquitination and degradation of the surfactant enzyme acyl-CoA: lysophosphatidylcholine acyltransferase I (LPCAT1). J Biol Chem **286:**2719–2727. http://dx.doi.org/10.1074/jbc.M110.192377.
29. **Zou C, Chen Y, Smith RM, Snavely C, Li J, Coon TA, Chen BB, Zhao Y, Mallampalli RK.** 2013. SCF^{Fbxw15} mediates histone acetyltransferase binding to origin recognition complex (HBO1) ubiquitin-proteasomal degradation to regulate cell proliferation. J Biol Chem **288:**6306–6316. http://dx.doi.org/10.1074/jbc.M112.426882.
30. **Chen BB, Coon TA, Glasser JR, McVerry BJ, Zhao J, Zhao Y, Zou C, Ellis B, Sciurba FC, Zhang Y, Mallampalli RK.** 2013. A combinatorial F box protein directed pathway controls TRAF adaptor stability to regulate inflammation. Nat Immunol **14:**470–479. http://dx.doi.org/10.1038/ni.2565.
31. **Inuzuka H, Gao D, Finley LW, Yang W, Wan L, Fukushima H, Chin YR, Zhai B, Shaik S, Lau AW, Wang Z, Gygi SP, Nakayama K, Teruya-Feldstein J, Toker A, Haigis MC, Pandolfi PP, Wei W.** 2012. Acetylation-dependent regulation of skp2 function. Cell **150:**179–193. http://dx.doi.org/10.1016/j.cell.2012.05.038.
32. **Weathington NM, Snavely CA, Chen BB, Zhao J, Zhao Y, Mallampalli RK.** 2014. Glycogen synthase kinase-3β stabilizes the interleukin (IL)-22 receptor from proteasomal degradation in murine lung epithelia. J Biol Chem **289:**17610–17619. http://dx.doi.org/10.1074/jbc.M114.551747.
33. **Lin HK, Wang G, Chen Z, Teruya-Feldstein J, Liu Y, Chan CH, Yang WL, Erdjument-Bromage H, Nakayama KI, Nimer S, Tempst P, Pandolfi PP.** 2009. Phosphorylation-dependent regulation of cytosolic localization and oncogenic function of Skp2 by Akt/PKB. Nat Cell Biol **11:**420–432. http://dx.doi.org/10.1038/ncb1849.
34. **Wu K, Katiyar S, Li A, Liu M, Ju X, Popov VM, Jiao X, Lisanti MP, Casola A, Pestell RG.** 2008. Dachshund inhibits oncogene-induced breast cancer cellular migration and invasion through suppression of interleukin-8. Proc Natl Acad Sci U S A **105:**6924–6929. http://dx.doi.org/10.1073/pnas.0802085105.

35. **Zhao J, Mialki RK, Wei J, Coon TA, Zou C, Chen BB, Mallampalli RK, Zhao Y.** 2013. SCF E3 ligase F-box protein complex SCF(FBXL19) regulates cell migration by mediating Rac1 ubiquitination and degradation. FASEB J **27:**2611–2619. http://dx.doi.org/10.1096/fj.12-223099.
36. **Tang X, Gao JS, Guan YJ, McLane KE, Yuan ZL, Ramratnam B, Chin YE.** 2007. Acetylation-dependent signal transduction for type I interferon receptor. Cell **131:**93–105. http://dx.doi.org/10.1016/j.cell.2007.07.034.
37. **Thakur RK, Yadav VK, Kumar P, Chowdhury S.** 2011. Mechanisms of non-metastatic 2 (NME2)-mediated control of metastasis across tumor types. Naunyn Schmiedebergs Arch Pharmacol **384:**397–406. http://dx.doi.org/10.1007/s00210-011-0631-0.
38. **Yoshida Y, Chiba T, Tokunaga F, Kawasaki H, Iwai K, Suzuki T, Ito Y, Matsuoka K, Yoshida M, Tanaka K, Tai T.** 2002. E3 ubiquitin ligase that recognizes sugar chains. Nature **418:**438–442. http://dx.doi.org/10.1038/nature00890.
39. **Zeng Z, Wang W, Yang Y, Chen Y, Yang X, Diehl JA, Liu X, Lei M.** 2010. Structural basis of selective ubiquitination of TRF1 by SCFFbx4. Dev Cell **18:**214–225. http://dx.doi.org/10.1016/j.devcel.2010.01.007.
40. **Berndsen CE, Wolberger C.** 2014. New insights into ubiquitin E3 ligase mechanism. Nat Struct Mol Biol **21:**301–307. http://dx.doi.org/10.1038/nsmb.2780.
41. **Zhou P, Howley PM.** 1998. Ubiquitination and degradation of the substrate recognition subunits of SCF ubiquitin-protein ligases. Mol Cell **2:**571–580. http://dx.doi.org/10.1016/S1097-2765(00)80156-2.
42. **Chen BB, Mallampalli RK.** 2013. F-box protein substrate recognition: a new insight. Cell cycle **12:**1009–1010. http://dx.doi.org/10.4161/cc.23071.
43. **D'Angiolella V, Donato V, Forrester FM, Jeong YT, Pellacani C, Kudo Y, Saraf A, Florens L, Washburn MP, Pagano M.** 2012. Cyclin F-mediated degradation of ribonucleotide reductase M2 controls genome integrity and DNA repair. Cell **149:**1023–1034. http://dx.doi.org/10.1016/j.cell.2012.03.043.
44. **Tang X, Orlicky S, Mittag T, Csizmok V, Pawson T, Forman-Kay JD, Sicheri F, Tyers M.** 2012. Composite low affinity interactions dictate recognition of the cyclin-dependent kinase inhibitor Sic1 by the SCF^{Cdc4} ubiquitin ligase. Proc Natl Acad Sci U S A **109:**3287–3292. http://dx.doi.org/10.1073/pnas.1116455109.
45. **Chang CL, Strahler JR, Thoraval DH, Qian MG, Hinderer R, Hanash SM.** 1996. A nucleoside diphosphate kinase A (nm23-H1) serine 120→glycine substitution in advanced stage neuroblastoma affects enzyme stability and alters protein-protein interaction. Oncogene **12:**659–667.
46. **Suryaraja R, Anitha M, Anbarasu K, Kumari G, Mahalingam S.** 2013. The E3 ubiquitin ligase Itch regulates tumor suppressor protein RASSF5/NORE1 stability in an acetylation-dependent manner. Cell Death Dis **4:**e565. http://dx.doi.org/10.1038/cddis.2013.91.